UNIVERSITY OF LIMERICK
OLLSCOIL LUIMNIGH

Self-healing hypercrosslinked metal–organic polyhedra (HCMOPs) membranes with antimicrobial activity and highly selective separation properties

Jinjin Liu, Wenjie Duan, Jie Song, Xiuxiu Guo, Zhifang Wang, Xinlei Shi, Jiajie Liang, Juan Wang, Peng Cheng, Michael J. Zaworotko, Zhenjie Zhang

Licence

Document Version

1

Citation for this work (HarvardUL)

Liu, J., Duan, W., Song, J., Guo, X., Wang, Z., Shi, X., Liang, J., Wang, J., Cheng, P., Zaworotko, M.J.and Zhang, Z. (2019) 'Self-healing hypercrosslinked metal–organic polyhedra (HCMOPs) membranes with antimicrobial activity and highly selective separation properties', available: https://hdl.handle.net/10344/8110 [accessed 24 Jul 2022].

Article

Self-healing Hypercrosslinked Metal–Organic Polyhedra (HCMOPs) Membranes with Antimicrobial Activity and Highly Selective Separation Properties

JinJin Liu, Wenjie Duan, Jie Song, Xiuxiu Guo, Zhifang Wang, Xinlei Shi, Jiajie Liang, Juan Wang, Peng Cheng, Yao Chen, Michael J. Zaworotko, and Zhenjie Zhang

Just Accepted

Self-healing Hypercrosslinked Metal–Organic Polyhedra (HCMOPs) Membranes with Antimicrobial Activity and Highly Selective Separation Properties

Jinjin Liu,[†] Wenjie Duan,[‡,§] Jie Song,[‡,§] Xiuxiu Guo,[†] Zhifang Wang,[†] Xinlei Shi,[‖] Jiajie Liang,[‖] Juan Wang,[†] Peng Cheng,[†] Yao Chen,*[,‡,§] Michael J. Zaworotko*[,⊥] and Zhenjie Zhang*[,†,‡]

[†] College of Chemistry, Nankai University, Tianjin, 300071, China

[‡] State Key Laboratory of Medicinal Chemical biology, Nankai University, Tianjin 300071, China

[⊥] Department of Chemical Sciences, Bernal Institute University of Limerick, Limerick V94T9PX, Republic of Ireland

[§] College of Pharmacy, Nankai University, Tianjin 300071, China

[‖] School of Materials Science and Engineering, Nankai University, Tianjin 300071, China

KEYWORDS: metal-organic polyhedra, membranes, self-healing, antimicrobial, separation

Dedicated to the 100th anniversary of Nankai University

ABSTRACT: Fabrication of hybrid membranes composed of porous materials embedded in polymer matrices is a subject of topical interest. Herein, we introduce a new class of hybrid membranes: hypercrosslinked metal-organic polyhedra (HCMOPs). These membranes are based upon soluble MOPs that can serve as high-connectivity nodes in hypercrosslinked polymer networks. HCMOPs spontaneously form macro-scale, defect-free, freestanding membranes and, thanks to the covalent cross-linking of MOPs, the resulting membranes possess multiple functionalities: strong water permeability; self-healing ability; antimicrobial activity; better separation and mechanical performance than pristine polyimine membranes. This study introduces a new concept for the design and fabrication of multi-functional membranes and also broadens the applications of MOPs.

INTRODUCTION

Membrane technologies can offer the advantages of easy-operation, low-cost and energy efficiency. It is therefore unsurprising that they have found widespread application in industrial processes including gas/liquid separation,[1,2] wastewater treatment,[3,4] biotechnology,[5] food engineering[6] and ion conduction.[7] Traditional polymer membranes tend to suffer limitations because of weak mechanical properties, the usual permeability-selectivity trade-off and their limited functionality.[8-10] Endowing membranes with multiple functionalities to improve membrane performance is a primary objective of the field.[11] For instance, self-healing ability will improve membrane durability against chemical or physical damages;[12-13] antibacterial properties will address biofouling by treating bacteria in water treatment.[14]

Incorporating fillers with multi-functionalities and intrinsic porosity into polymer matrices to fabricate mixed-matrix membranes (MMMs) can address some of the limitations of traditional polymer membranes.[10,15] However, MMMs are typically fabricated by adding insoluble solid fillers such as zeolites, metal–organic frameworks (MOFs)[16] and covalent organic frameworks (COFs)[17] and tend to suffer from interfacial defects because of poor compatibility between fillers and polymer matrix. This often causes agglomeration and precipitation of fillers during membrane formation and leads to poor membrane performance.[18,19] Exploring new membrane fabrication techniques and fillers that can supersede traditional porous materials is therefore an attractive proposition.

As the subunits (i.e. supermolecular building blocks) of MOFs, metal–organic polyhedra (MOPs) inherit certain features of MOFs such as ordered structure,[20,21] tunable pore sizes,[22,23] high porosity,[24] good stability[25,26] and designable functionality.[27-32] More importantly, MOPs can offer excellent processability arising from their high solubility[33-35] in certain solvents.[36] This in turn enables facile post-synthetic modification of MOPs to promote interactions with other materials such as polymers.[37-41] However, until now, only few approach (i.e. MMMs or photopolymerization) have been used to incorporate MOPs into polymers in order to fabricate hybrid membranes (Figure S1).[42-45] Unfortunately, these hybrid membranes may still suffer from leaching of MOPs, poor mechanical properties and limited functionality. Herein, we address these issues by introducing a new concept: hypercrosslinked MOPs (HCMOPs). We report herein that soluble MOPs can serve as co-monomers to produce macro-scale, defect-free, freestanding HCMOP membranes with self-

1

healing ability, antibacterial activity and outstanding mechanical and separation performance (Scheme 1). This new generation of hybrid MOP membranes offers the potential to address the limits of the current generation of MOP-based MMMs.

RESULTS AND DISCUSSION

Design and synthesis of soluble MOPs with polymerizable groups (e.g. –NH$_2$, -CH=CH$_2$) and selecting appropriate crosslinking polymer matrixes are key to fabricating HCMOP membranes. Highly stable zirconium-based MOPs have attracted increasing attention due to their porosity, functionality, outstanding stability and good solubility.[25] Zr-MOPs can easily adjust their pore size via changing the linker ligand length while retaining the same skeleton. Moreover, functional groups such as amino and vinyl moieties can be readily introduced into Zr-MOPs.[46-48] After having been functionalized with polymerizable groups, Zr-MOPs are suitable to serve as high-connectivity nodes. Polyimines are mechanically tough cross-linking polymers which form freestanding membranes under ambient conditions.[49] The reversible nature of imine bonds means that polyimines can possess outstanding performance such as reshaping, self-healing and antimicrobial performance.[50-51] Herein, we detail how HCMOPs can be formed using Zr-MOPs with six amino groups that polymerize with aldehydes to form polyimine-MOP hybrid materials (Scheme 1).

Scheme 1. The strategy introduced herein fabricates HCMOP membranes via introducing functionalized MOPs as porous co-monomers.
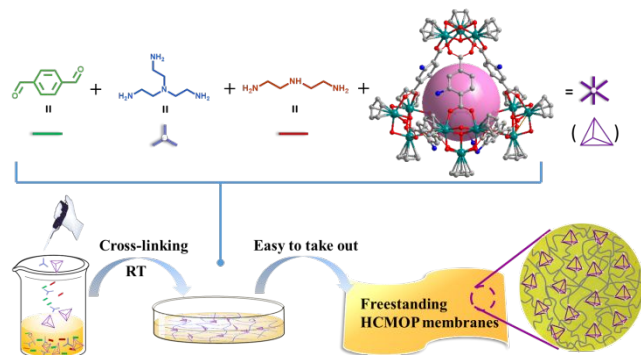
The MOP used herein, **MOP-1**, was synthesized according to the literature procedure by reaction of zirconium (IV) with 2-aminoterephthalic acid (H$_2$BDC-NH$_2$).[46] Powder X-ray diffraction (PXRD) analyses (Figure S2) verified the bulk purity of as-synthesized **MOP-1**. In **MOP-1**, four trinuclear Zr clusters serve as 3-connected vertexes that are linked by BDC-NH$_2$ to form a tetrahedral cage with accessible inner space for guest molecules (Figure 2A and S3).[47] Notably, **MOP-1** exhibits high solubility in methanol (~3.3 mg/mL) (Table S2). **MOP-1** in methanol was studied by ^{1}H NMR (Figure S4) and ultra performance liquid chromatography-quadrupole mass spectrometry (UPLC-Q-TOF-MS), which confirmed the presence of intact cationic tetrahedral cages in methanol. It is consistent with the literature that the peaks (m/z of 938.2015, 1250.6029 and 1874.3933) with continuous charge states from

+2 to +4 correspond to [M-6Cl-2H]$^{4+}$, [M-6Cl-3H]$^{3+}$, and [M-6Cl-4H]$^{2+}$ ions, respectively (Figure S5).[25] In addition, the experimental isotopic distribution patterns of each charge state are in good agreement with the theoretically calculated values based on the chemical composition of **MOP-1**.[25] Moreover, UPLC-Q-TOF-MS analysis proved that **MOP-1** was intact in dissolution/precipitation recycling experiments (Figure S6).

As shown in Scheme 1, a multi-component condensation reaction was employed to prepare HCMOPs via ambient polymerization of diethylene triamine, tris(2-aminoethyl)amine, terephthaldehyde and **MOP-1** in mixed organic solvents (1:1:8, v/v/v, CH$_2$Cl$_2$/EtOAc/MeOH) at room temperature (Figure 1A). Diethylene triamine, tris(2-aminoethyl)amine and **MOP-1** can serve as 2-, 3- and 6-connected nodes, respectively, to react with terephthaldehyde to generate hypercrosslinked networks linked with imine bonds. After allowing the volatiles to evaporate slowly, a series of **HCMOP-1** variants (a = 0.1, b = 0.2, c = 0.4, representing the different weight ratios of **MOP-1**/terephthaldehyde) membranes were obtained by varying **MOP-1** content (Figure S7). When the weight ratio of MOP and terephthaldehyde was below 0.4, uniform, transparent, highly flexible, freestanding **HCMOP-1** membranes were formed, but when the MOP was in excess, nonuniform membranes with rough surfaces formed. It is possible that the MOPs reacted with terephthaldehyde to form crosslinked MOPs or discrete species which hindered embedding with the polyimine (Figure S8). We determined that **HCMOP-1** membranes offer outstanding mechanical performance. The dry **HCMOP-1** membrane can be repeatedly bent, twisted or stretched without damage and lift a steel object >200 g (Figure 1B; Videos S1 and S2). Wet **HCMOP-1** membranes were found to be softer and more flexible and could be elongated by a factor of ~0.24. Moreover, **HCMOP-1** membranes possessed excellent reshaping ability derived from the water-induced malleability.[49] A dry membrane was immersed into water for 3 h to generate a wet, pliable membrane which can be easily reshaped (Figure 1C). After drying, **HCMOP-1** membrane maintained its new shape and exhibited good mechanical properties (e.g. support a steel object >200 g without significant flexure).
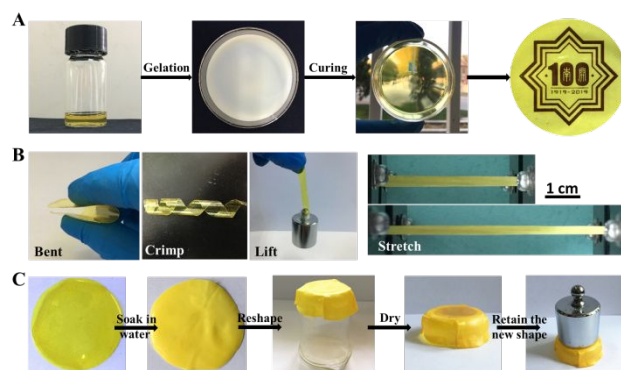
Figure 1. (A) The process to produce **HCMOP-1** membranes. (B) Mechanical performance of an **HCMOP-1** membrane. (C) Demonstration of the reshaping ability of an **HCMOP-1** membrane.

FT-IR was used to validate the formation of the imine backbone in the copolymerization reaction of **HCMOP-1** (Figure S9-S12). After copolymerization, a new absorption band at 1640 cm^{-1} corresponding to the C=N stretch of imine bond became prominent in the FT-IR spectra, while the C=O stretch absorption band at 1683 cm^{-1} for the aldehyde was barely detectable. These results support that condensation of aldehyde groups to form imine linkers occurred during polymerization. In order to confirm covalent bonding between **MOP-1** and the polyimine matrix, **MOP-1** was reacted with benzaldehyde in the same synthesis condition as **HCMOP-1**. ^{1}H NMR data confirmed reaction of **MOP-1** with aldehyde as indicated by the appearance of new peaks of 7.3~7.5 ppm (Figure S13). The UPLC-Q-TOF-MS results provide support for **MOP-1** being decorated with six phenylmethanimine groups (peaks at m/z of 938.2015, 1250.6029 and 1874.3933) with charge states from +2 to +4 corresponding to [M-6Cl-2H]$^{4+}$, [M-6Cl-3H]$^{3+}$, and [M-6Cl-4H]$^{2+}$ ions, respectively (Figure S14).

Additionally, we designed and synthesized a MOPs@polymer variant by adding an isostructural MOP, **MOP-1'** (terephthalate linkers)[47] (Figure 2A, S15 and S16) during the synthesis procedure used for **HCMOP-1**. Although **MOP-1'** also exhibits good solubility in methanol, it cannot form covalent bonds with polyimine due to the lack of reactive groups (i.e. amino) and therefore leaches out in certain solvents. Leaching experiments were conducted via soaking **HCMOP-1** and **MOP-1'@polyimine** in water with sonication for 2 hours. Inductively coupled plasma mass spectrometry (ICP-MS) was used to test whether or not the MOPs had leached out from the membranes. The Zr concentration was determined to be 0.048 μg/mL for **MOP-1'@polyimine** whereas <0.001 μg/mL was detected for **HCMOP-1**. These results demonstrate an advantage of HCMOPs *vs.* traditional MMMs.

The uniformity and quality of HCMOP membranes were evaluated by scanning electron microscopy (SEM) and energy-dispersive x-ray (EDX). SEM images (Figure 2B and S17) revealed that the HCMOP membranes possess smooth surfaces and compact packing without defects on the surface and cross-sections. EDX analysis and mapping (Figure 2C, S18 and S19) revealed that **MOP-1** was homogenously dispersed throughout the membranes as indicated by Zr distribution. The thickness of HCMOP membranes was conveniently adjusted via changing the reactant amount.

We next demonstrated that the HCMOP approach can be applied using other MOPs. 3,3'-diamino-1,1'-biphenyl-4,4'-dicarboxylic acid (H$_2$BPDC-NH$_2$) was employed to replace H$_2$BDC-NH$_2$ and afford a new MOP, **MOP-2'** (Figure S20 and S21). The solubility of **MOP-2'** in methanol is lower (0.8 mg/mL) and this affected its utility to fabricate uniform HCMOP membranes. In order to improve its solubility, bis(n-butylcyclopentadienyl)zirconium dichloride was used instead of bis(cyclopentadienyl)zirconium dichloride to afford **MOP-2** (Figure S22). The alkyl chains significantly increase solubility (36.8 mg/mL of **MOP-2** in methanol). Single-crystal X-ray diffraction analysis revealed that **MOP-2** and **MOP-2'** are the expected isoreticular analogues of **MOP-1** (Figure 2A and Table S1). ^{1}H NMR and UPLC-Q-TOF-MS revealed the presence of intact **MOP-2** cations in methanol (Figure S23 and S24). UPLC-Q-TOF-MS analysis indicated that **MOP-2**

was intact in dissolution/precipitation recycling experiments (Figure S25). A series of **HCMOP-2** membranes were then fabricated (Figure S7) under the procedure used for **HCMOP-1**. SEM images demonstrated the uniform and defect-free surface of **HCMOP-2** (Figure S17). EDX analysis and mapping revealed the existence of uniformly dispersed **MOP-2** in the resulting membrane (Figure S18 and S19).
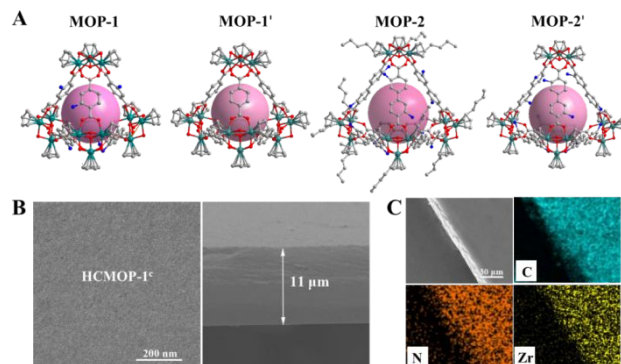
Figure 2. (A) Crystal structures of Zr-MOPs. Color code: C, gray; O, red; N, blue; Zr, green. The free spaces in the structure were depicted as the inserted pink sphere. For clarity, H atoms were omitted. (B) Top view (left) and cross-section (right) SEM images of the freestanding **HCMOP-1^c** membranes. (C) EDX mapping of **HCMOP-1^c**.

Functionality such as self-healing ability and antimicrobial properties will greatly enhance a membrane's performance and potential applications in industry.[12-14] Firstly, in order to prove if our HCMOP membranes possess self-healing ability attributed to the dynamic nature of imine/amine exchange reactions (Figure S26),[52] HCMOP membranes were cut with a 1.8 mm scratch by a surgical blade at room temperature. After the membranes with cracks were placed into a 60 °C oven for 5 hours, the resulting cracks were healed without melting (Figure 3A and S27). This self-healing behavior can be ascribed to the polymer chain movement and imine/amine exchange reaction resulting from the reversible nature of imine bonds.[50] Meanwhile, stress–strain experiments revealed that HCMOP membranes recovered their mechanical performance after self-healing (Figure S28). These results indicate that HCMOPs represent the first examples of self-healing polymer-MOP hybrid membranes. Antimicrobial activity of HCMOPs can be attributed to the interaction between the electronegative charges on the microbial cell surface and protonated amino groups from unreacted amino groups and decomposition of imine bonds.[53] As reported in the literature, this electrostatic interaction leads to internal osmotic imbalances, and also results in the leakage of intracellular electrolytes and other low molecular weight proteinaceous constituents, which consequently inhibits the growth of the microorganisms.[54] Two bacteria (*Staphylococcus aureus* (*S. aureus*) and *Escherichia coli* (*E. coli*)) and two fungi (*Cryptococcus neoformans* (*C. neoformans*) and *Saccharomyces cerevisiae* (*S. cerevisiae*)) were selected to evaluate antimicrobial activity. We found that all HCMOP membranes possess good antimicrobial activity, especially for fungus, as indicated by the inhibition zone (Figure 3B, S29, S30 and Table S3) and minimum inhibitory concentrations (MICs) (Table S4).

3

We also found that the flux of the HCMOP membranes was 150 L h^{-1} m^{-2} bar^{-1} (Table S5), significantly higher than that of commercial polymeric membranes (typically in the range of 10-50 L h^{-1} m^{-2} bar^{-1}).[55,56] Thus, HCMOP membranes could be suitable for treating pathogens from contaminated water. *S. aureus* and *C. neoformans* (1.0×10^7 CFU/mL) were selected as representative bacteria and fungus. No pathogen colonies formed on the plate after filtering through the HCMOP membrane (Figure S31) for >15 cycles, indicative of excellent pathogen separation efficiency and reusability (Figure S32). Moreover, HCMOP membranes not only removed pathogens but they also possessed good durability resulted from their self-healing ability. As demonstrated in Figure 3C, the damaged membrane fully recovers its separation performance after seal-healing. These results indicate that HCMOP membranes have potential to treat pathogen contamination in water resources.
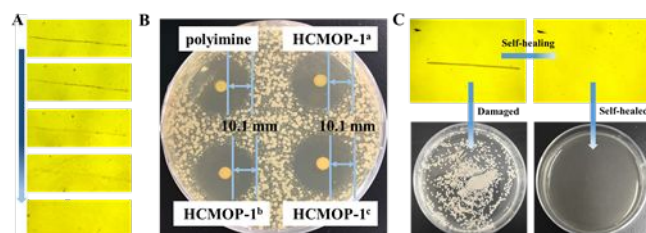
Figure 3. (A) Optical microscopy images of the self-healing process of damaged **HCMOP-1^c** membrane. (B) The inhibition zone of polyimine and **HCMOP-1** against *C. neoformans*. (C) The filtration experiment of *C. neoformans* by a damaged **HCMOP-1^c** membrane (left) and a self-healed **HCMOP-1^c** membrane (right).

Further studies found that HCMOP membranes not only inherit advantages from the polymer component, but also enhance membrane performance such as mechanical strength and selectivity attributable to the presence of MOPs. Mechanical properties of **HCMOP-1** membranes were evaluated by stress–strain experiments. As shown in Figure 4A, the Young's modulus of **HCMOP-1** was significantly enhanced when gradually increasing MOP content from 0 to 0.4 (Figure S33). Among these membranes, **HCMOP-1^c** achieved the highest Young's modulus of 1721 MPa, almost 1.5 times as much as the pristine polyimine membrane (1192 MPa). That each **MOP-1** cage can serve as a 6-connected node to provide high connectivity can explain this increase in strength. We also prepared a series of **MOP-1'@polyimine** MMMs as comparison (Figure S34), and found that ultimate stress and Young's modulus of **MOP-1'@polyimine** showed the reverse trend *vs.* **HCMOP-1**, i.e. decreasing strength with increasing **MOP-1'** content from 0 to 0.4. These results further indicate that **MOP-1** strongly bonds with polyimines via covalent bonds. Additionally, stress–strain experiments revealed that wet **HCMOP-1** membranes possessed improved toughness over dry membranes (Figure 4B, S35 and Video S3), possibly because water induces hydrolysis of polyimines and facilitates imine/amine exchange reactions (Figure S26).[46] Notably, **HCMOP-1^c** membranes possessed higher Young's modulus in both dry and wet states compared with pristine polyimine. **HCMOP-2** membranes also exhibited the same

trend as **HCMOP-1** with enhanced mechanical properties (Figure S36 and S37). Overall, the mechanical performance of HCMOP membranes was much better than the pristine polymeric membrane and traditional **MOP-1'@polyimine** MMMs.
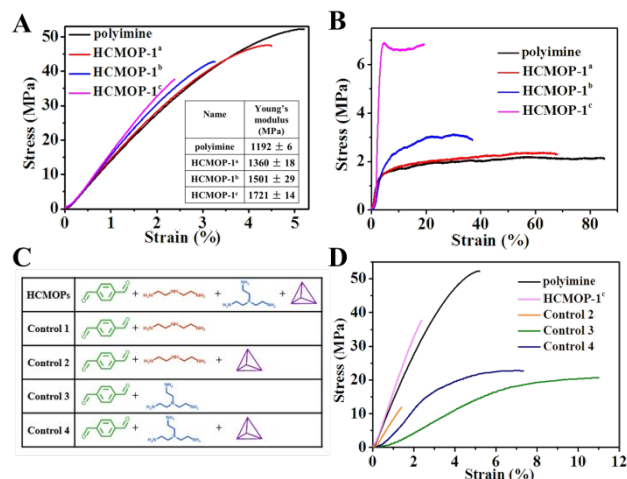

Figure 4. (A) Stress-strain curves and Young's modulus of dry **HCMOP-1** membranes. (B) Stress-strain curves of wet **HCMOP-1** membranes. (C) Reactants of control experiments. (D) Stress-strain curves of control 2, 3 and 4 compared with polyimine and **HCMOP-1^c**.

To address the role of two specific amines in the preparation of hypercrosslinked membranes, we designed and fabricated four types of membranes with different reactants as control experiments and studied their relationship between components and mechanical properties (Figure 4C, S38 and Table S6). As shown in Figure 4D, control 1 of terephthaldehyde and diethylene triamine barely formed a freestanding membrane and it was found to exhibit poor mechanical behavior (stress-strain curve was not testable), possibly because it formed a linear polymer instead of a hypercrosslinked polymer network. After introducing **MOP-1**, the mechanical strength of the formed membrane was significantly improved in control 2. We also found that membranes in control 3 and 4 with tris(2-aminoethyl)amine possessed good ductility but low mechanical strength, which will limit their utility. On the contrary, **HCMOP-1^c** membranes synthesized via adding both diethylene triamine and tris(2-aminoethyl)amine possessed the highest Young's modulus. Hence, the two specific amines were essential to generate hypercrosslinked membranes with good mechanical properties.

MOP-1 and **-2** can provide intrinsic positive charges (zeta potential of +38.4 and +62.2 mV, respectively) to hybrid systems. Therefore, HCMOP membranes should inherit properties from the cationic nature of the MOPs and could therefore exhibit distinct separation performance compared with pristine neutral polyimine membranes. We selected eight water-soluble dyes with different charges, including anionic dyes: Brilliant Yellow (BY), Chicago Sky Blue 6B (CSB) and Congo Red (CR); neutral dyes: Nile Red (NR), Rhodamine 6G (R6G) and Vitamin B12 (VB12); cationic dyes: Rhodamine B (RB) and Basic Brown (BB) (Figure S39 and Table S7). The

4

rejection results revealed that HCMOPs had remarkably better rejection performance for anionic dyes rather than neutral dyes and cationic dyes (Table S8) and that the effect was significantly improved with increased MOP content, e.g. the rejection ratio for BY improved from 76% to >99% (Figure 5A). To further study the selectivity of HCMOPs for dyes of different charges, HCMOP membranes were subjected to two kinds of mixed feed of BY(anionic)/RB(cationic) or BY(anionic)/R6G(neutral). In these systems, all HCMOP membranes rejected BY and allowed RB or R6G to pass (Figure 5B, 5C and S40-S42). The adsorption capacity (Q_t) was monitored for each membrane *vs*. time (Figure S43).[57] **HCMOP-1^c** displayed the fastest adsorption initially and the highest Q_t to BY ratio. The adsorption rate and capacity for RB of **HCMOP-1^c** were much lower (Figure 5D). These results are consistent with the expected electrostatic interactions between HCMOPs and dye molecules. The reusability of HCMOP membranes was investigated by testing the separation of BY; no BY could be detected even after six filtration cycles (Figure S44). These results revealed that HCMOP membranes exhibit much better selective separation and mechanical performance than pristine polyimine membranes.
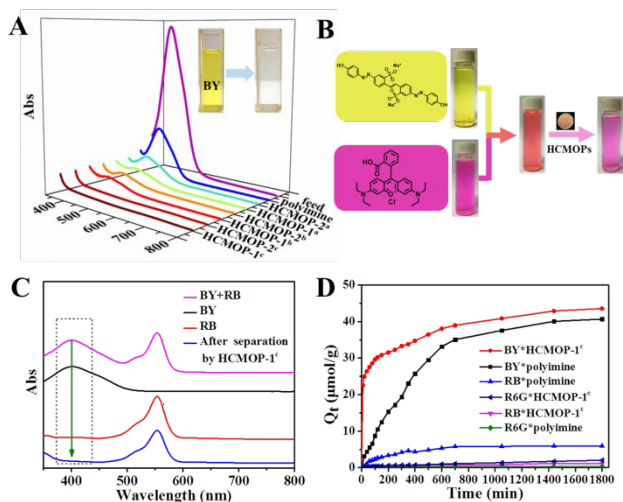
Figure 5. (A) UV-Vis spectra of BY solution Feed and Permeate. (B) Photograph to show the selective separation of BY from BY/RB mixture. (C) UV-Vis spectra of selective sieving of BY from BY/R6G mixture by **HCMOP-1^c** membrane. (D) Adsorption capacity Q_t versus time curves for the adsorption of BY, RB and R6G at 20 °C ('*' represents 'adsorbed on').

CONCLUSION

In conclusion, we introduce a new generation of hypercrosslinked membranes through use of soluble MOPs as cross-linking co-monomers that serve as high connectivity nodes. The HCMOP approach affords macroscale, defect-free, freestanding hybrid membranes which inherit features from both the MOP (e.g. cationic nature and permanent porosity) and the polymer (e.g. self-healing ability, antimicrobial activity, high water permeability and good processability) components. In addition, the introduction of MOPs into

polymers was found to significantly enhance mechanical properties, selective separation and water permeability. The self-healing ability and antimicrobial activity further supports the potential utility of HCMOP membranes (e.g. to kill pathogens and improve the durability of membranes) for treating pathogen contamination in water resources. The HCMOP membranes reported herein not only surpass traditional MOP-based MMMs, but also demonstrate advantages over polymer-MOP hybrid materials which mostly form gels or powders.[25,35-39] We believe that the approach reported herein for fabricating HCMOP membranes will be applicable to other soluble porous materials that can serve as monomers and other polymer matrices.

ASSOCIATED CONTENT

Supporting Information

The Supporting Information is available free of charge on the ACS Publications website. Material, methods, synthesis procedures of ligands, MOPs and HCMOPs, UV−Vis, FT-IR, ^{1}H NMR, PXRD, crystal structure data, gas sorption isotherms, SEM, EDX, mass spectrometry, zeta potential, stress and strain curves (PDF)

AUTHOR INFORMATION

Corresponding Author

*chenyao@nankai.edu.cn
*Michael.Zaworotko@sspc.ie
*zhangzhenjie@nankai.edu.cn

Notes

The authors declare no competing financial interest.

REFERENCES

(1) Bernardo, P.; Drioli, E.; Golemme, G. Membrane Gas Separation: A Review/State of the Art. *Ind. Eng. Chem. Res.* **2009**, *48* (10), 4638-4663.

(2) Li, X.; Liu, Y.; Wang, J.; Gascon, J.; Li, J.; Van Der Bruggen, B. Metal–Organic Frameworks Based Membranes for Liquid Separation. *Chem. Soc. Rev.* **2017**, *46* (23), 7124-7144.

(3) Han, Y.; Xu, Z.; Gao, C. Ultrathin Graphene Nanofiltration Membrane for Water Purification. *Adv. Funct. Mater.* **2013**, *23* (29), 3693-3700.

(4) Consortium, T. I. T.; Giacomini, K. M.; Huang, S.-M.; Tweedie, D. J.; Benet, L. Z.; Brouwer, K. L. R.; Chu, X.; Dahlin, A.; Evers, R.; Fischer, V.; Hillgren, K. M.; Hoffmaster, K. A.; Ishikawa, T.; Keppler, D.; Kim, R. B.; Lee, C. A.; Niemi, M.; Polli, J. W.; Sugiyama, Y.; Swaan, P. W.; Ware, J. A.; Wright, S. H.; Yee, S. W.; Zamek-Gliszczynski, M. J.; Zhang, L. Membrane Transporters in Drug Development. *Nat. Rev. Drug Discov.* **2010**, *9*, 215-236.

(5) Meng, F.; Chae, S.-R.; Drews, A.; Kraume, M.; Shin, H.-S.; Yang, F. Recent Advances in Membrane Bioreactors (MBRs): Membrane Fouling and Membrane Material. *Water Res.* **2009**, *43* (6), 1489-1512.

(6) Joscelyne, S. M.; Trägårdh, G. Food Emulsions Using

5

Membrane Emulsification: Conditions for Producing Small Droplets. *J. Food Eng.* **1999**, *39* (1), 59-64.

(7) He, G.; Li, Z.; Zhao, J.; Wang, S.; Wu, H.; Guiver, M. D.; Jiang, Z. Nanostructured Ion-Exchange Membranes for Fuel Cells: Recent Advances and Perspectives. *Adv. Mater.* **2015**, *27* (36), 5280-5295.

(8) Robeson, L. M. The Upper Bound Revisited. *J. Memb. Sci.* **2008**, *320* (1-2), 390-400.

(9) Dechnik, J.; Gascon, J.; Doonan, C. J.; Janiak, C.; Sumby, C. J. Mixed-Matrix Membranes. *Angew. Chem. Int. Ed.* **2017**, *56* (32), 9292-9310.

(10) Park, H. B.; Kamcev, J.; Robeson, L. M.; Elimelech, M.; Freeman, B. D. Maximizing the Right Stuff: The Trade-Off between Membrane Permeability and Selectivity. *Science* **2017**, *356* (6343), eaab0530.

(11) Bai, H.; Liu, Z.; Sun, D. D. A Hierarchically Structured and Multifunctional Membrane for Water Treatment. *Appl. Catal. B-Environ.* **2012**, *111-112*, 571-577.

(12) Chen, X.; Dam, M. A.; Ono, K.; Mal, A.; Shen, H.; Nutt, S. R.; Sheran, K.; Wudl, F. A Thermally Re-Mendable Cross-Linked Polymeric Material. *Science* **2002**, *295* (5560), 1698-1702.

(13) Fang, W.; Liu, L.; Li, T.; Dang, Z.; Qiao, C.; Xu, J.; Wang, Y. Electrospun N-Substituted Polyurethane Membranes with Self-Healing Ability for Self-Cleaning and Oil/Water Separation. *Chem. Eur. J.* **2016**, *22* (3), 878-883.

(14) Aryanti, P. T. P.; Sianipar, M.; Zunita, M.; Wenten, I. G. Modified Membrane with Antibacterial Properties. *Membr. Water Treat.* **2017**, *8* (5), 463-481.

(15) Qiu, S.; Xue, M.; Zhu, G. Metal–Organic Framework Membranes: From Synthesis to Separation Application. *Chem. Soc. Rev.* **2014**, *43* (16), 6116-6140.

(16) Denny, M. S.; Kalaj, M.; Bentz, K. C.; Cohen, S. M. Multicomponent Metal–Organic Framework Membranes for Advanced Functional Composites. *Chem. Sci.* **2018**, *9* (47), 8842-8849.

(17) Biswal, B. P.; Chaudhari, H. D.; Banerjee, R.; Kharul, U. K. Chemically Stable Covalent Organic Framework (COF) - Polybenzimidazole Hybrid Membranes: Enhanced Gas Separation through Pore Modulation. *Chem. Eur. J.* **2016**, *22* (14), 4695-4699.

(18) Zornoza, B.; Tellez, C.; Coronas, J.; Gascon, J.; Kapteijn, F. Metal Organic Framework Based Mixed Matrix Membranes: An Increasingly Important Field of Research with a Large Application Potential. *Microporous Mesoporous Mater.* **2013**, *166*, 67-78.

(19) Campbell, J.; Székely, G.; Davies, R. P.; Braddock, D.C.; Livingston, A. G. Fabrication of Hybrid Polymer/Metal Organic Framework Membranes: Mixed Matrix Membranes versus in Situ Growth. *J. Mater. Chem. A* **2014**, *2* (24), 9260-9271.

(20) Eddaoudi, M.; Kim, J.; Wachter, J. B.; Chae, H. K.; O'Keeffe, M.; Yaghi, O. M. Porous Metal−Organic Polyhedra: 25 Å Cuboctahedron Constructed from 12 $Cu_2(CO_2)_4$ Paddle-Wheel Building Blocks. *J. Am. Chem. Soc.* **2001**, *123* (18), 4368-4369.

(21) Abourahma, H.; Coleman, A. W.; Moulton, B.; Rather, B.; Shahgaldian, P.; Zaworotko, M. J. Hydroxylated Nanoballs: Synthesis, Crystal Structure, Solubility and Crystallization on Surfaces. *Chem. Commun.* **2001**, 2380-2381.

(22) Dalgarno, S. J.; Power, N. P.; Atwood, J. L. Metallo-Supramolecular Capsules. *Coord. Chem. Rev.* **2008**, *252* (8-9), 825-841.

(23) Kang, Y. H.; Liu, X. D.; Yan, N.; Jiang, Y.; Liu, X. Q.; Sun, L. B.; Li, J. R. Fabrication of Isolated Metal–Organic Polyhedra in Confined Cavities: Adsorbents/Catalysts with Unusual Dispersity and Activity. *J. Am. Chem. Soc.* **2016**, *138* (19), 6099-6102.

(24) Li, J.-R.; Zhou, H.-C. Bridging-Ligand-Substitution Strategy for the Preparation of Metal–Organic Polyhedra. *Nat. Chem.* **2010**, *2*, 893-898.

(25) Liu, G.; Di Yuan, Y.; Wang, J.; Cheng, Y.; Peh, S. B.; Wang, Y.; Qian, Y.; Dong, J.; Yuan, D.; Zhao, D. Process-Tracing Study on

the Postassembly Modification of Highly Stable Zirconium Metal–Organic Cages. *J. Am. Chem. Soc.* **2018**, *140* (20), 6231-6234.

(26) Carné-sánchez, A.; Craig, G. A.; Larpent, P.; Guillerm, V.; Urayama, K.; Maspoch, D.; Furukawa, S. A Coordinative Solubilizer Method to Fabricate Soft Porous Materials from Insoluble Metal‐Organic Polyhedra. *Angew. Chem. Int. Ed.* **2019**, *58* (19), 6347-6350.

(27) Liu, T.; Liu, Y.; Xuan, W.; Cui, Y. Chiral Nanoscale Metal–Organic Tetrahedral Cages: Diastereoselective Self-Assembly and Enantioselective Separation. *Angew. Chem. Int. Ed.* **2010**, *49* (24), 4121-4124.

(28) Zheng, Y. -R.; Zhao, Z.; Wang, M.; Ghosh, K.; Pollock, J. B.; Cook, T. R.; Stang, P. J. A Facile Approach toward Multicomponent Supramolecular Structures: Selective Self-Assembly via Charge Separation. *J. Am. Chem. Soc.* **2010**, *132* (47), 16873-16882.

(29) Bilbeisi, R. A.; Clegg, J. K.; Elgrishi, N.; Hatten, X. de; Devillard, M.; Breiner, B.; Mal, P.; Nitschke, J. R. Subcomponent Self-Assembly and Guest-Binding Properties of Face-Capped $Fe_4L_4^{8+}$ Capsules. *J. Am. Chem. Soc.* **2012**, *134* (11), 5110-5119.

(30) Zhang, Y.; Gan, H.; Qin, C.; Wang, X.; Su, Z.; Zaworotko, M. J. Self-Assembly of Goldberg Polyhedra from a Concave $[WV_5O_{11}(RCO_2)_5(SO_4)]^{3-}$ Building Block with 5-Fold Symmetry. *J. Am. Chem. Soc.* **2018**, *140* (50), 17365-17368.

(31) Lal, G.; Derakhshandeh, M.; Akhtar, F.; Spasyuk, D. M.; Lin, J.-B.; Trifkovic, M.; Shimizu, G. K. H. Mechanical Properties of a Metal–Organic Framework Formed by Covalent Cross-Linking of Metal–Organic Polyhedra. *J. Am. Chem. Soc.* **2019**, *141* (2), 1045-1053.

(32) Kang, Y. -H.; Yan, N.; Gao, Z. -Y.; Tan, P.; Jiang, Y.; Liu, X. -Q.; Sun, L. -B. Controllable Construction of Metal‐Organic Polyhedra in Confined Cavities via in Situ Site-Induced Assembly. *J. Mater. Chem. A* **2017**, *5* (11), 5278-5282.

(33) Kawano, M.; Kobayashi, Y.; Ozeki, T.; Fujita, M. Direct Crystallographic Observation of a Coordinatively Unsaturated Transition-Metal Complex in Situ Generated within a Self-Assembled Cage. *J. Am. Chem. Soc.* **2006**, *128* (20), 6558-6559.

(34) Dai, F.-R.; Qiao, Y.; Wang, Z. Designing Structurally Tunable and Functionally Versatile Synthetic Supercontainers. *Inorg. Chem. Front.* **2016**, *3* (2), 243-249.

(35) Carné-Sánchez, A.; Craig, G. A.; Larpent, P.; Hirose, T.; Higuchi, M.; Kitagawa, S.; Matsuda, K.; Urayama, K.; Furukawa, S. Self-Assembly of Metal–Organic Polyhedra into Supramolecular Polymers with Intrinsic Microporosity. *Nat. Commun.* **2018**, *9* (1), 2506.

(36) Ma, J.; Ying, Y.; Yang, Q.; Ban, Y.; Huang, H.; Guo, X.; Xiao, Y.; Liu, D.; Li, Y.; Yang, W.; Zhong, C. Mixed-Matrix Membranes Containing Functionalized Porous Metal–Organic Polyhedrons for the Effective Separation of CO_2-CH_4 Mixture. *Chem. Commun.* **2015**, *51* (20), 4249-4251.

(37) Sun, Y.; Chen, C.; Stang, P. J. Soft Materials with Diverse Suprastructures via the Self-Assembly of Metal–Organic Complexes. *Acc. Chem. Res.* **2019**, *52* (3), 802-817.

(38) Gu, Y.; Alt, E. A.; Wang, H.; Li, X.; Willard, A. P.; Johnson, J. A. Photoswitching Topology in Polymer Networks with Metal–Organic Cages as Crosslinks. *Nature* **2018**, *560* (7716), 65-69.

(39) Zhukhovitskiy, A. V; Zhong, M.; Keeler, E. G.; Michaelis, V. K.; Sun, J. E. P.; Hore, M. J. A.; Pochan, D. J.; Griffin, R. G.; Willard, A. P.; Johnson, J. A. Highly Branched and Loop-Rich Gels via Formation of Metal–Organic Cages Linked by Polymers. *Nat. Chem.* **2016**, *8*, 33-41.

(40) Foster, J. A.; Parker, R. M.; Belenguer, A. M.; Kishi, N.; Sutton, S.; Abell, C.; Nitschke, J. R. Differentially Addressable Cavities within Metal–Organic Cage-Cross-Linked Polymeric Hydrogels. *J. Am. Chem. Soc.* **2015**, *137* (30), 9722-9729.

(41) Hosono, N.; Kitagawa, S. Modular Design of Porous Soft Materials via Self-Organization of Metal–Organic Cages. *Acc. Chem. Res.* **2018**, *51* (10), 2437-2446.

(42) Perez, E. V; Balkus, K. J.; Ferraris, J. P.; Musselman, I. H.

Metal–Organic Polyhedra 18 Mixed-Matrix Membranes for Gas Separation. *J. Memb. Sci.* **2014**, *463*, 82-93.

(43) Yun, Y. N.; Sohail, M.; Moon, J. -H.; Kim, T. W.; Park, K. M.; Chun, D. H.; Park, Y. C.; Cho, C. -H.; Kim, H. Defect-Free Mixed-Matrix Membranes with Hydrophilic Metal–Organic Polyhedra for Efficient Carbon Dioxide Separation. *Chem. Asian J.* **2018**, *13* (6), 631-635.

(44) Zhao, C.; Wang, N.; Wang, L.; Sheng, S.; Fan, H.; Yang, F.; Ji, S.; Li, J.; Yu, J. Functionalized Metal–Organic Polyhedra Hybrid Membranes for Aromatic Hydrocarbons Recovery. *AIChE J.* **2016**, *62* (10), 3706-3716.

(45) Xie, X.-Y.; Wu, F.; Liu, X.; Tao, W.-Q.; Jiang, Y.; Liu, X.-Q.; Sun, L.-B. Photopolymerization of Metal–Organic Polyhedra: An Efficient Approach to Improve the Hydrostability, Dispersity, and Processability. *Chem. Commun.* **2019**, *55* (44), 6177-6180.

(46) Nam, D.; Huh, J.; Lee, J.; Kwak, J. H.; Jeong, H. Y.; Choi, K.; Choe, W. Cross-Linking Zr-Based Metal–Organic Polyhedra via Postsynthetic Polymerization. *Chem. Sci.* **2017**, *8* (11), 7765-7771.

(47) Liu, G.; Ju, Z.; Yuan, D.; Hong, M. In Situ Construction of a Coordination Zirconocene Tetrahedron. *Inorg. Chem.* **2013**, *52* (24), 13815-13817.

(48) Xing, W.-H.; Li, H.-Y.; Dong, X.-Y.; Zang, S.-Q. Robust Multifunctional Zr-Based Metal–Organic Polyhedra for High Proton Conductivity and Selective CO_2 Capture. *J. Mater. Chem. A* **2018**, *6* (17), 7724-7730.

(49) Taynton, P.; Yu, K.; Shoemaker, R. K.; Jin, Y.; Qi, H. J.; Zhang, W. Heat- or Water-Driven Malleability in a Highly Recyclable Covalent Network Polymer. *Adv. Mater.* **2014**, *26* (23), 3938-3942.

(50) Li, H.; Bai, J.; Shi, Z.; Yin, J. Environmental Friendly Polymers Based on Schiff-Base Reaction with Self-Healing, Remolding and Degradable Ability. *Polymer* **2016**, *85*, 106-113.

(51) Vashi, K.; Naik, H. B. Synthesis of Novel Schiff Base and Azetidinone Derivatives and Their Antibacterial Activity. *E -J. Chem.* **2004**, *1* (5), 272-275.

(52) Kathan, M.; Kovaříček, P.; Jurissek, C.; Senf, A.; Dallmann, A.; Thünemann, A. F.; Hecht, S. Control of Imine Exchange Kinetics with Photoswitches to Modulate Self-Healing in Polysiloxane Networks by Light Illumination. *Angew. Chem. Int. Ed.* **2016**, *55* (44), 13882-13886.

(53) Anush, S. M.; Vishalakshi, B.; Kalluraya, B.; Manju, N. Synthesis of Pyrazole-Based Schiff Bases of Chitosan: Evaluation of Antimicrobial Activity. *Int. J. Biol. Macromol.* **2018**, *119*, 446–452.

(54) Sabaa, M. W.; Elzanaty, A. M.; Abdel-Gawad, O. F.; Arafa, E. G. Synthesis, Characterization and Antimicrobial Activity of Schiff Bases Modified Chitosan-Graft-Poly (Acrylonitrile). *Int. J. Biol. Macromol.* **2018**, *109*, 1280-1291.

(55) Cheng, S.; Oatley, D. L.; Williams, P. M.; Wright, C. J. Characterisation and Application of a Novel Positively Charged Nanofiltration Membrane for the Treatment of Textile Industry Wastewaters. *Water Res.* **2012**, *46* (1), 33-42.

(56) Wang, Z.; Yu, Q.; Huang, Y.; An, H.; Zhao, Y.; Feng, Y.; Li, X.; Shi, X.; Liang, J.; Pan, F.; Cheng, P.; Chen, Y.; Ma, S.; Zhang, Z. PolyCOFs: A New Class of Freestanding Responsive Covalent Organic Framework Membranes with High Mechanical Performance. *ACS Cent. Sci.* **2019**, https://doi.org/10.1021/acscentsci.9b00212.

(57) Fu, G.; Su, Z.; Jiang, X.; Yin, J. Photo-Crosslinked Nanofibers of Poly (Ether Amine) (PEA) for the Ultrafast Separation of Dyes through Molecular Filtration. *Polym. Chem.* **2014**, *5* (6), 2027-2034.
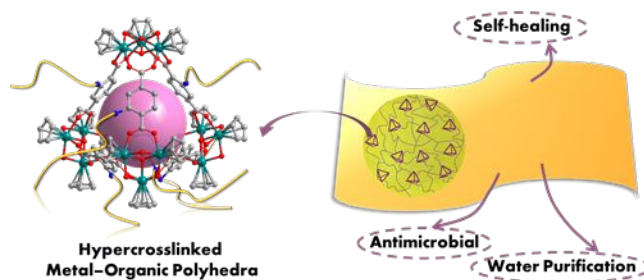
7